AUTOMATIC MURA DETECTION SYSTEM FOR LIQUID CRYSTAL DISPLAY PANELS

Li-Te Fang***, Hsin-Chia Chen***, I-Chieh Yin***, Sheng-Jyh Wang***,

Chao-Hua Wen*, Cheng-Hang Kuo**,

Taiwan TFT-LCD Association, Taiwan*
Industrial Technology Research Institute, Taiwan**
Institute of Electronics, National Chiao Tung University, Taiwan***

E-mail: phalex.ee92g@nctu.edu.tw

ABSTRACT

In this paper, we propose an automatic inspection system, which can automatically detect four types of muras on an LCD panel: cluster mura, v-band mura, rubbing mura, and light leakage mura. To detect cluster muras, the Laplacian of Gaussian (LOG) filter is used. A multi-resolution approach is proposed to detect cluster muras of different scales. To speed up the processing speed, this multi-resolution approach is actually implemented in the frequency domain. To detect v-band muras, we check the variation tendency of the projected 1-D intensity profile. Then, v-band muras are detected by identifying these portions of the 1-D profile where a large deviation occurs. To detect rubbing muras, we designed a frequency mask to detect distinct components in the frequency domain. To detect light leak muras, we apply image mirroring over the boundary parts and adopt the same LOG filter that has been used in detecting cluster muras. All four types of mura detection are integrated together in an efficient way and simulation results demonstrate that this system is indeed very helpful in detecting mura defects.

Keywords: Laplacian of Gaussian, Mura defect, Mura detection, SEMU, automatic inspection.

1 INTRODUCTION

As TFT-LCD (Thin Film Transistor Liquid Crystal Display) devices get more and more popular in display market, the inspection of LCD quality has been receiving increasing attention. So far, most inspection methods depend on the perception of human eyes. However, there are many disadvantages in human inspection: high labor power, inconsistent detection, and limitations in visual sensitivity. Hence, automatic inspection based on machine vision could be another option for the inspection of LCD panels.

In this paper, we propose an automatic inspection system for the inspection of visual defects on TFT-LCD panels. These visual defects are usually called muras in the literature. They are defined as visible imperfections on an active LCD display screen. A typical mura usually appears as a low-contrast and non-uniform region and is typically larger than a single pixel [1]. The causes of muras are due to the imperfection manufactures of various components or foreign particles within the liquid crystal. Several efforts have already been spent to classify these defects and to establish the evaluation standards [1-2]. Several detection algorithms, on the other hand, have also been proposed in the literature [3-8].

In this paper, we focus on the detection of four types of muras. The contents of this paper are organized as follows. In Section 2, we introduce the inspection procedure of our mura inspection system and propose several mura detection algorithms. Conclusions are then given in Section 3.

2 INSPECTION PROCEDURE

The inspection system is shown in Figure 1. It consists of three major parts: 1) the LCD panel under test, 2) a CCD camera, and 3) a personal computer to execute mura detection algorithms. The inspection procedure is described as

Machine Vision Applications in Industrial Inspection XIV, edited by Fabrice Meriaudeau, Kurt S. Niel,
Proc. of SPIE-IS&T Electronic Imaging, SPIE Vol. 6070, 60700G, © 2006 SPIE-IS&T · 0277-786X/06/$15

follows. The LCD panel is first placed on the equipment vertically. This panel is driven by a pattern generator to generate patterns of constant gray level. Then, a high-resolution digital camera takes a few FOS (Front-Of-Screen) images and these FOS images are transmitted to the computer to be inspected by our mura inspection algorithms. The CCD camera has a 14-bit dynamic range and a spatial resolution of 2048 by 2048 pixels. The detection flow chart of this mura detection system is illustrated in Figure 1(b).

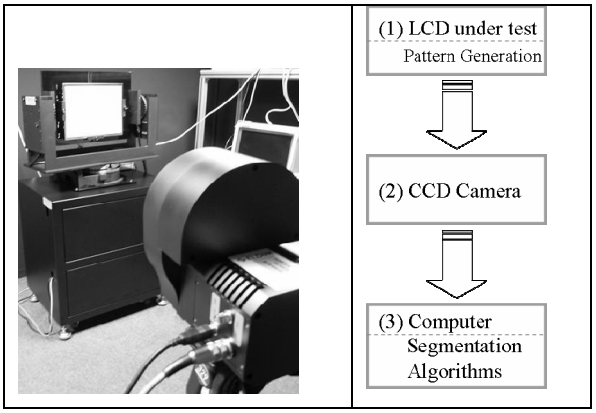

Figure 1. (a) mura inspection system;
(b) inspection flowchart.

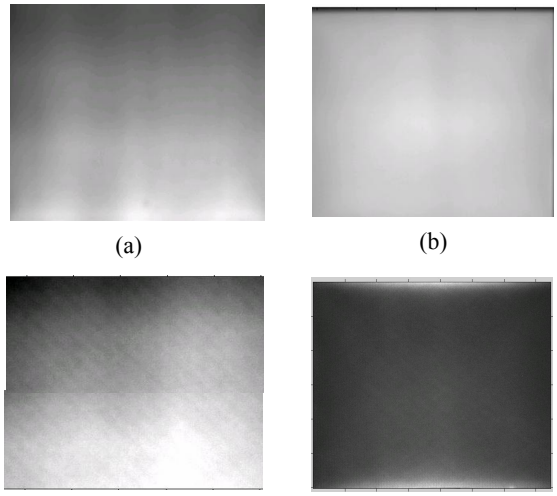

Figure 2. (a) Cluster Mura; (b) Vertical Band Mura;
(c) Rubbing Mura; (d) Light Leak Mura.

Among various kinds of mura defects, our mura inspection system focuses on the detection of four typical types of mura defects: cluster mura, vertical-band mura (v-band mura), rubbing mura, and light leak mura (LL mura). A cluster mura usually appears as a cluster of dark or bright points in a localized area, as shown at the central bottom of Figure 2(a); v-band mura appears as a wide, vertical stripe with different brightness with respect to the background, as shown in the middle of Figure 2(b); rubbing mura usually appears as tiled lines with a 45-degree angle spreading over a large region, as shown in Figure 2(c); and light leak mura appears at the boundary of LCD panels, as shown on the top and bottom of Figure 2(d).

The inspection procedure of our system is illustrated in Figure 3. The LCD panel is first driven by patterns of constant gray level. The image is transmitted to the computer to be processed by the detection algorithms. The detection procedure consists of two major tracks. In one track, v-band muras are to be detected in the spatial domain via a curve fitting method. In the other track, the boundary of the FOS image is first padded with mirror images that are to be used for the detection of light-leak muras. The image is then transformed into the frequency domain to detect cluster muras, rubbing muras, and light-leak muras. The results of all these four mura detection algorithms are then combined together to generate the final detection report.

2.1 Inspection of Cluster Mura

Cluster Mura usually appears as a cluster of bright or dark points in a localized area [9]. Generally speaking, there are two types of cluster mura: round-type cluster mura and line-type cluster mura, as shown in Figure 4(a) and (b). A major cause of cluster mura is due to dust or particles coming into some layers of LCD panel. Poor LCD manufactory process may also produce this type of defects.

In [9], we proposed a 2-D LOG (Laplacian of Gaussian) filters to detect cluster muras. The LOG filter is designed to match the shapes of cluster mura, with the optimal threshold being determined based on the SEMU formula [9]. To detect round-type cluster muras, the round-type LOG filter is chosen to be

$$filter_{LOG}^{Round}(x, y) = \left(\nabla_{xx} + \nabla_{yy}\right) N(x, y; 0, \sigma_x, \sigma_y), \qquad (1)$$

where $N(x,y;0,\sigma_x,\sigma_y)=\frac{1}{2\pi\sigma_x\sigma_y}e^{-(\frac{x^2}{2\sigma_x^2}+\frac{y^2}{2\sigma_y^2})}$ denotes a 2-D Gaussian function with zero mean and standard deviations σ_x and σ_y, respectively. If we choose $\sigma_x = \sigma_y = \sigma$, then there is only one parameter to be assigned by the users. On the other hand, to detect a horizontal line-type cluster mura, the LOG filter is chosen to be

$$filter_{LOG}^{\text{Rectangular}}(x,y)=(\nabla_{yy})N(x,y;0,\sigma_x,\sigma_y). \qquad (2)$$

If the ratio of σ_x/σ_y is fixed, there is only one parameter left [9]. Similarly, to detect a vertical line-type mura, we can use an operator similar to (2) with ∇_{yy} being replaced by ∇_{xx}.

Figure 5 shows these two types of LOG operator and Figure 4(c) and (d) show the corresponding detection results, where these detected muras are marked in red.

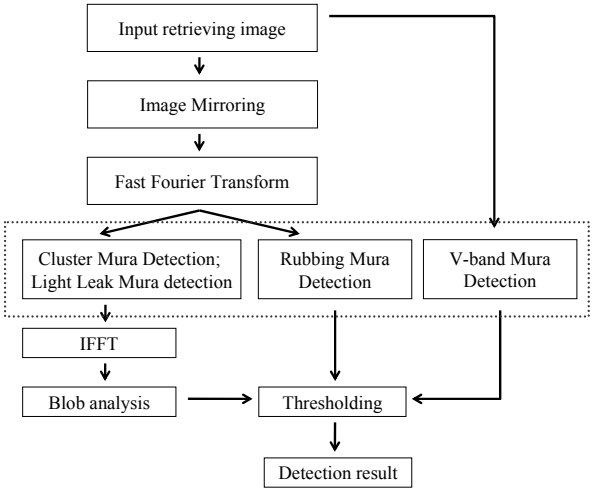

Figure 3. Flow Chart of mura detection algorithms

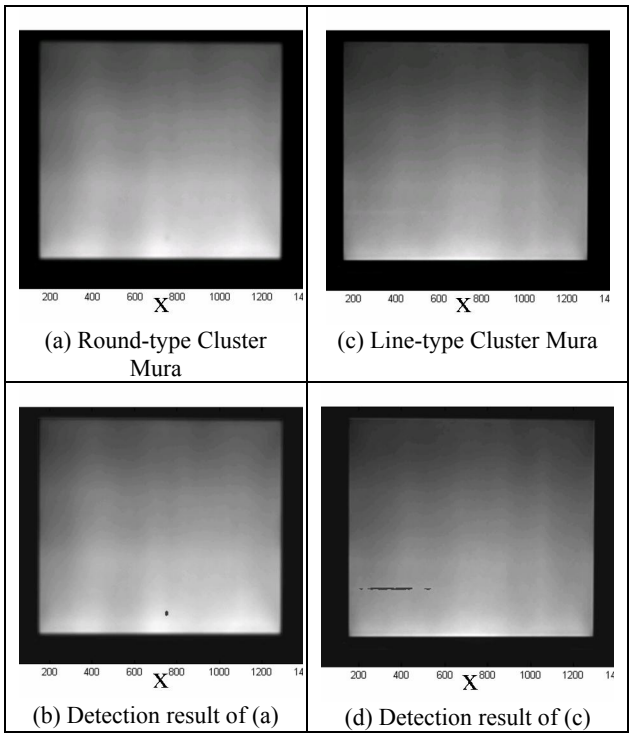

Figure 4. Cluster Mura

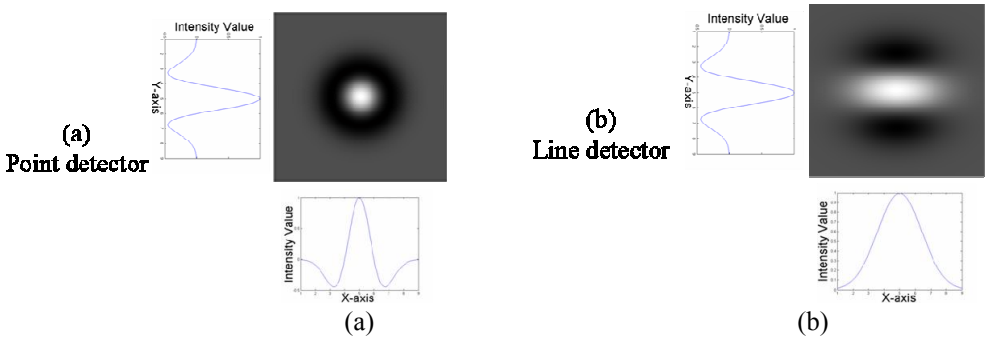

(a) (b)

Figure 5. (a) Round-type LOG operator ; (b) Line-type LOG operator.

Even though the method proposed in [9] is quite effective in detecting cluster muras, the execution time of spatial convolution could be a problem. In the detection of cluster muras, we need to inspect muras of different sizes. As we increase the size of the LOG operator to detect cluster muras of larger size, the computation load of the convolution operation increases exponentially. To deal with this kind of problem, we convert the operation from spatial domain to frequency domain. In theory, convolution of two digital patterns in the spatial domain is equivalent to multiplication of their counterparts in the frequency domain. More explicitly, we have

$$\Im\{f(x,y) * g(x,y)\} = \Im\{f(x,y)\} \cdot \Im\{g(x,y)\} \qquad (3)$$

or

$$f(x,y) * g(x,y) = \Im^{-1}\{\Im\{f(x,y)\} \cdot \Im\{g(x,y)\}\}, \quad (4)$$

where * denotes the convolution operation and $\Im\{.\}$ denotes the Fourier transform operation. Hence, to perform the convolution operation, we may compute the Fourier transforms of the original image and the LOG operator first, multiply their transforms together, and then perform inverse Fourier transformation over their multiplication product to get the final convolution result.

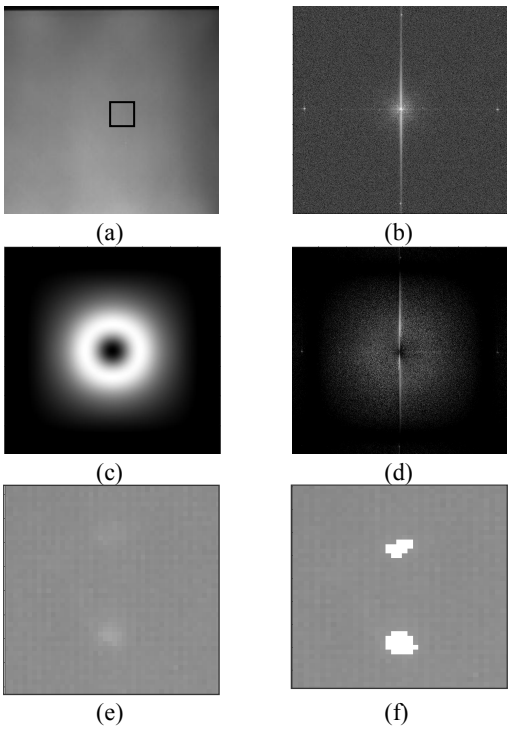

Figure 6. Example of cluster mura detection
(a) original image; (b) FFT of the original image;
(c) FFT of an LOG filter; (d) product of (b) and (c);
(e) zoomed image of the red rectangle area marked in (a);
(f) detection result of (e).

Figure 6 illustrates an example of this process. Figure 6(a) shows the FOS image of an LCD panel and Figure 6(b) shows its Fourier transform. Here, we apply FFT (Fast Fourier Transform) for the computation of Fourier transform. Figure 6(c) shows the Fourier transform of a round-type LOG filter with $\sigma_x = \sigma_y = \sigma = 1$. Figure 6(d) shows the product of Figure 6(b) and (c). After computing the multiplication product, we perform inverse Fourier transform to get the corresponding convolution result. A threshold is then selected to detect cluster muras. Figure 6(e) shows a zoomed image of the red rectangle area marked in Figure 6(a). Figure 6(f) shows the corresponding detection result. These

detected pixels are grouped into blobs. Based on the Semu formula [2], we further check the semu value of these detected blobs to determine whether these blobs are perceivable to human eyes.

As mentioned above, different sizes of LOG filters are used to detect cluster muras of different scales. Here we adopt a multi-resolution approach to detect cluster muras of various sizes. Note that we only need to perform the Fourier transform of the original image once. To detect cluster muras of different sizes, we only need to multiply the Fourier transform of the original image with the Fourier transforms of different LOG filters. These multiplication products are then converted back to the spatial domain, respectively. All these convolution results are then merged in a proper way to generate the final results. Figure 7 illustrates an example for the proposed multi-resolution cluster mura detection. Figure 7 (a) contains 8 synthesized muras, with radius being 5, 10, 15, 20, 25, 30, 35, and 40, respectively. The luminance of the background is zero. For this example, we apply two LOG filters with σ = 10 and 30, respectively. In theory, it can be deduced that, for each LOG filter, the convolution result will reach its maximum magnitude when the size of mura matches to the size of the LOG filter [9]. Figure 7 (b) shows the convolution result by using the LOG filter with σ = 10. It can be seen that the convolution result does reach its maximum magnitude (represented in red) at the mura with radius 10. Figure 7 (c) shows a similar result when we use the LOG filter with σ = 30. Moreover, both LOG filters are normalized to have their positive parts summed to 1 and negative parts summed to -1. With this normalization, when the intensity difference between the mura and the surrounding background is kept the same, the maximum magnitude of the convolution result for different LOG filters will also be normalized to be the same.

After performing multiple convolutions with LOG filters of different scales, we merge all convolution results by calculating at each pixel the maximum magnitude of all convolution results. That is, we calculate

$$\text{result}(x,y) = \max(\text{result}_1(x,y), \text{result}_2(x,y), ...) \quad (5)$$

where $\text{result}_i(x,y)$ denotes the convolution result at (x,y) with the use of the ith LOG filter. Figure 7(d) shows the final result based on (5). Figure 7(e)~(g) show the detection results of Figure 7 (b)~(d) by setting the threshold to be 100. As expected, it can be seen that the smaller LOG filter detects only small muras, while the larger LOG filter detects only large muras. However, with the proposed multi-resolution approach, all sizes of mura defects can be correctly detected.

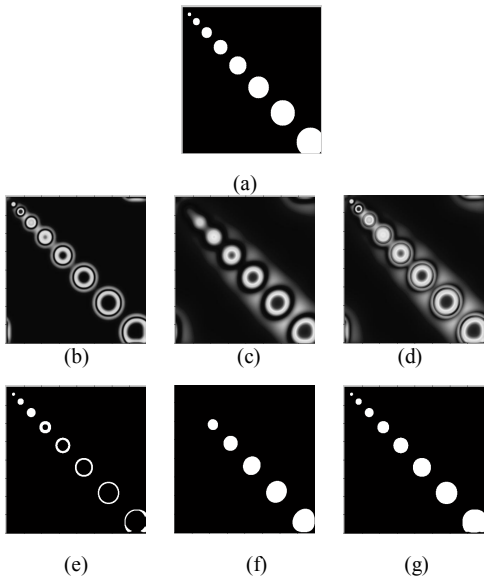

Figure 7 Multi-resolution cluster mura detection
(a) test image;
(b) result by using an LOG filter with σ =10;
(c) result by using an LOG filter with σ =30;
(d) maximization of (b) and (c);
(e)~(g) detection results of (b)~(d), respectively, with threshold =100.

2.2 Inspection of V-band Mura

V-band mura appears as a wide, vertical stripe with different brightness with respect to the background. The cause of V-Band Mura usually comes from non-uniform thickness of components, such as non-uniform thickness of glasses in the cell unit. This type of mura spreads over a large area. Hence, it is difficult to detect v-band muras based simply on local operator. To detect V-band mura, we check the variation tendency of the projected 1-D intensity profile. Figure 8(a) shows an FOS image. We first vertically project the 2-D image data into a 1-D intensity profile, shown as the blue dotted line in Figure 8(b). In the projected profile, significant intensity deviations indicate the existence of V-band muras. To detect large intensity deviation, we analyze the variation tendency of the projected profile by checking the profile curvature. Here, we adopt the zero-crossing points on the profile curvature to indicate the turning points of variation tendency. Based on these zero-crossing points, a 2nd-order curve fitting is performed to generate a smooth approximation of the projected profile, shown as the cyan line in Figure 8(b). Figure 8(c) shows the difference between the smooth approximating profile and the original profile. The difference is smoothed by Gaussian filter to suppress noise. Red points indicate local minimums while green points indicate local maximums. To determine whether there is a visible v-band mura, we calculate at each local extreme the intensity difference between that extreme and its adjacent local extremes, indicated as the red line in Figure 8(c). This intensity difference indicates how serious a local deviation is, as indicated in Figure 8(d). If the difference is above a pre-selected threshold, that local deviation is detected as a v-band mura. In our experiments, the threshold is set to be 0.015, empirically. Figure 8(e) shows the final detection result, with the cyan box indicating the area of the detected V-band muras.

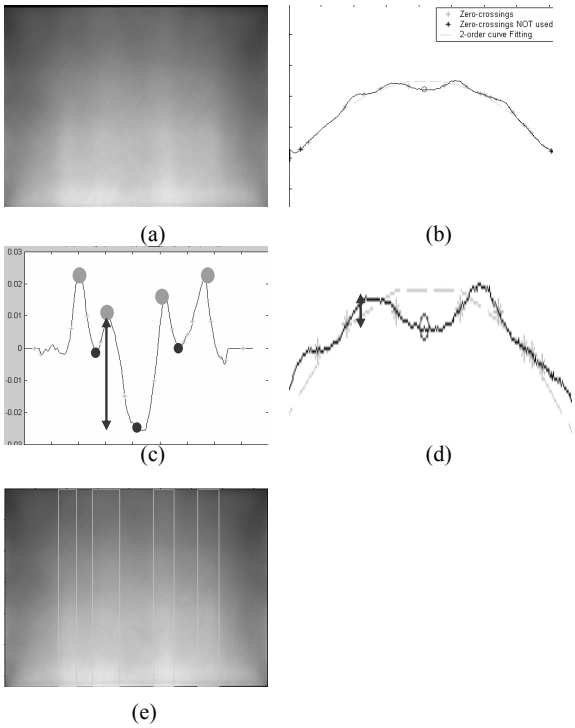

Figure 8. Example of v-band mura detection
(a) original FOS imag e;
(b) projected 1-D profile, zero-crossing points, and fitted curve;
(c) difference between the 1-D projection and the fitted curve;
(d) illustration of intensity deviation;
(e) detection result.

2.3 Inspection of Rubbing Mura

During the manufacturing of LCD panels, the rubbing process is a process to control the arrangement of liquid crystals. However, during this process, dust or particles may cause rubbing muras. Poor rubbing process or polluted rubbing cloth may also cause this kind of defects. Figure 9(a) shows a typical rubbing mura on the FOS image of an LCD panel. These

rubbing lines appear along the diagonal direction. Because these Rubbing lines appear as a periodic pattern, we may apply frequency-domain analysis to the extraction of rubbing muras.

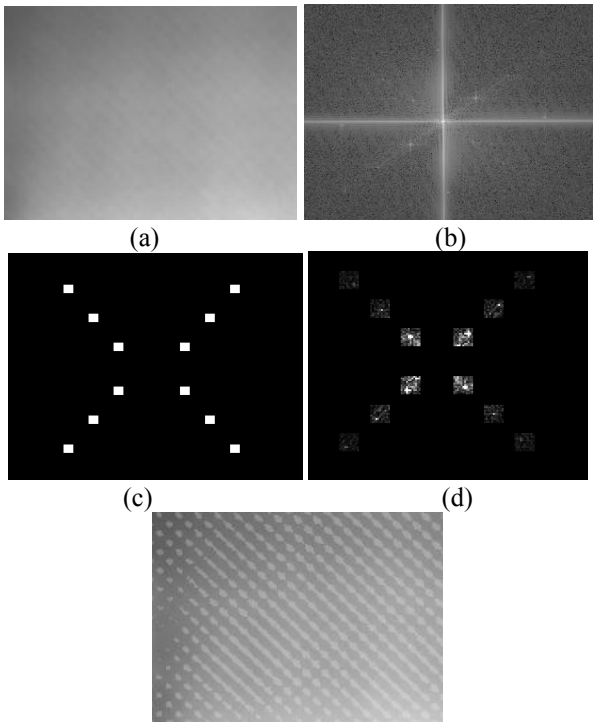

Figure 9. (a) FOS image with Rubbing Mura;
(b) FFT of (a);
(c) frequency mask;
(d) masked frequency components;
(e) detected rubbing mura.

Figure 9(b) shows the FFT of the FOS image with rubbing mura. The center of Figure 9(b) represents the dc component and the two axes represent the frequency axes along the vertical and horizontal directions. Due to the existence of rubbing mura, there appear a few bright points in Figure 9(b) that correspond to the strong periodic components in the FOS image. In our experiments, rubbing muras tend to appear at the same frequency. With this observation, we presume the same manufacturing process will produce the same type of rubbing mura. Hence, we explicitly design a frequency mask as shown in Figure 9(c) to sift out unnecessary frequency components. Moreover, in the design of the frequency mask, we also preserve the 2^{nd} and 3^{rd} harmonic components. Figure 9(d) shows the masked frequency contents. If we transform the masked frequency components back to the spatial domain via inverse FFT, we can get the red pattern as shown in Figure 9(e). This pattern does correspond to the rubbing mura in Figure 9(a). Hence, to detect rubbing muras, we may simply check whether there are distinct components in the masked frequency components. Here, we check the sum of power to detect the existence of distinct components. In Table 1, we show the comparison between the JND (Just Noticeable Difference) value and the sum of power of the masked frequency components. These subjective JND values are determined by professional LCD panel inspectors, who had been well trained to inspect the visual quality of LCD panels. A mura with "JND-value =1.5" indicates that the contrast of that mura is about 1.5 times of the JND level, subjectively. Table 1 indicates that the JND-value of a rubbing mura is basically proportional to the power sum. As a result, we can select a threshold, shown as the red line in Table 1, to determine whether there is a rubbing mura in the FOS image of an LCD panel. Note that the thresholding is performed in the frequency domain and there is no need to convert the masked frequency components back to the spatial domain.

Table 1. JND value inspected by inspectors versus power sum in the masked frequency components

LCD number	JND value by inspector	Sum of power in frequency domain
LCD1		16801
LCD2		18544
LCD3		30912
LCD4		33492
LCD5		41728
LCD6		43381
LCD7		58281
LCD8	1.8	129056
LCD9	2.2	155356
LCD10	1.8	169928
LCD11	1.7	176191
LCD12	2.1	195643
LCD13	2.1 L92 1.8	274746
LCD14	2.4 L92 2.2-2.3	275137

Threshold

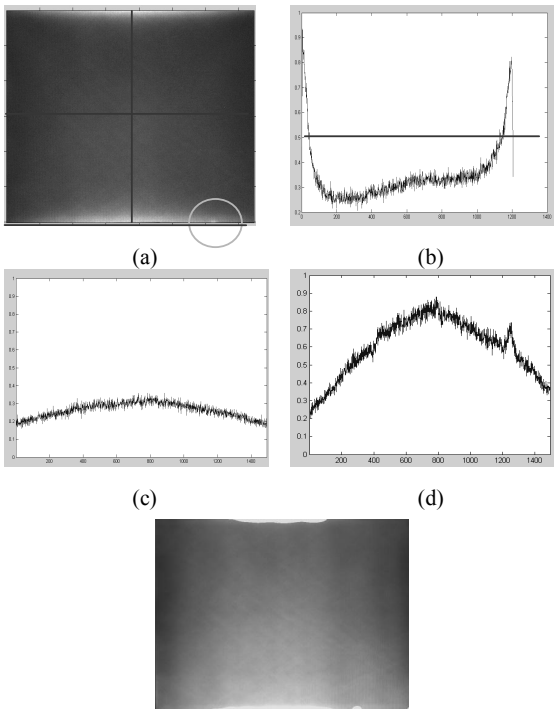

(a) (b) (c) (d) (e)

Figure 10. (a) FOS image with light leakage muras; (b) 1-D intensity profile along the vertical red line in (a); (c) 1-D intensity profile along the central horizontal line in (a); (d)1-D intensity profile along the bottom horizontal line in (a); (e) detection result.

2.4 Inspection of Light Leak Mura

Light leakage muras usually appears at the boundary regions of an LCD panel. An ideal LCD panel should have no visible bright area around the boundaries of the panel if the screen is in fully dark. However, light leakage may occur at the boundaries due to misalignment during manufacturing. The non-uniform distribution of brightness enhancement film in the boundary region may also produce this kind of mura defect. Figure 10 (a) shows an example of light leakage

mura. We can easily see that both the upper side and the bottom side of the FOS image appear brighter than the other regions. Figure 10 (b) shows the 1-D intensity profile along the red vertical line in Figure 10(a). The intensity values at both ends are much higher than that in the center. Figure 10(c) and Figure 10 (d) show the 1-D intensity profiles along the two red horizontal lines in Figure 10(a). It can be seen that the intensity value across the center part is roughly flat, while the intensity value along the bottom boundary changes quite dramatically.

To detect light leakage muras, we also adopt the aforementioned LOG filter that has been used in the detection of cluster muras. However, since light leakage muras always occur at boundaries of the FOS image, we need to manipulate the boundary regions properly before we apply the LOG operator. For example, as shown in Figure 11(b), above the top boundary of the FOS image, we pad a mirror image of that part. We also pad mirror images around the bottom, left, and right boundaries of the FOS image. After the padding, a light leakage mura appears just like a line-type cluster mura and we can simply apply a line-type LOG filter as shown in Figure 11(c) to detect it. The process would be the same as that in detecting cluster muras and the detection result of Figure 10(a) is shown in Figure 10(e).

3 CONCLUSION

To detect four types of muras, an automatic inspection system was proposed. This system can detect cluster mura, v-band mura, rubbing mura, and light leakage mura. To detect cluster muras, a multi-resolution approach based on the LOG filter is used. To speed up the processing speed, this multi-resolution approach is implemented in the frequency domain. To detect v-band muras, we check the variation tendency of the projected 1-D intensity profile. To detect rubbing muras, we designed a frequency mask to detect distinct components in the frequency domain. To detect light leak muras, we apply image mirroring over the boundary parts and adopt the same LOG filter that has been used in detecting cluster muras. All four types of mura detection are integrated together in an efficient way. Simulation results demonstrate that this system is indeed very helpful in detecting mura defects.

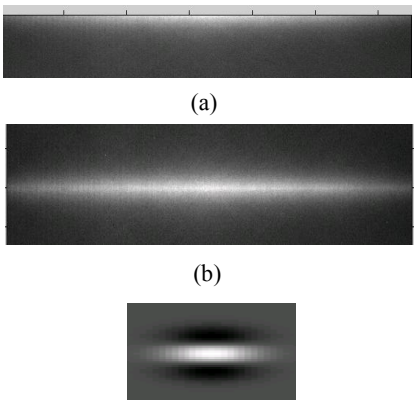

(a) (b) (c)

Figure 11. (a) Top boundary area of Figure 10(a);
(b) padded on the top of (a) with a mirror image;
(c) applied line-type LOG filter.

4 REFERENCES

[1] Video Electronics Standards Association (VESA): Flat Panel Display Measurements Standard, version 2.0, p.78.

[2] Semiconductor Equipment and Materials International (SEMI) standard, "New Standard: Definition of Measurement Index (SEMU) for Luminance Mura in FPD Image Quality Inspection," draft number: 3324, pp. 1-6, 2002.

[3] Y. Mori, K. Tanahashi, and S. Tsuji, "Quantitative Evaluation of Visual Performance of Liquid Crystal Displays," SPIE Proceedings of the Algorithms and Systems for Optical Information Processing, vol. 4113, pp. 242-249, 2000.

[4] Y. Mori, R. Yoshitake, T. Tamura, T. Yoshizawa and S. Tsuji, “Evaluation and Discrimination Method of "mura" in Liquid Crystal Displays by Just Noticeable Difference Observation,” Proceedings of SPIE, vol. 4902, pp. 715-722, 2002.

[5] W. K. Pratt, S. S. Sawkar, and K. O'Reilly, “Automatic Blemish Detection in Liquid Crystal Flat Panel Displays,” Proceeding of SPIE, vol. 3306, pp. 2-13, 1998.

[6] V. Gibour and T. Leroux, “Automated, Eye-like Analysis of Mura Defects,” Proceedings of SID, pp. 1440-1443, 2003.

[7] D. G. Lee, I. H. Kim, M. C. Jeong, B. K. Oh, and W. Y. Kim, “Mura Analysis Method by Using JND Luminance And the SEMU Definition,” Proceedings of SID, pp. 1467-1470, 2003.

[8] T. Tamura, M. Baba and T. Furuhata, “Effect of the Background Luminance on Just Noticeable Difference Contrast of ‘Mura’ in LCDs,” Proceedings of SID, pp. 1527-1530, 2003.

[9] Hsin-Chia Chen, Li-Te Fang, Sheng-Jyh Wang, “LOG Filter Based Inspection of Cluster Mura and Vertical Band Mura on Liquid Crystal Displays”, Proceedings of SPIE, Vol. 5679, Jan. 2005.